Journal of Colloid and Interface Science 662 (2024) 99–108

Contents lists available at ScienceDirect

Journal of Colloid And Interface Science

journal homepage: www.elsevier.com/locate/jcis

Regular Article

Morphology and thermal transitions of self-assembled NIPAM-DMA copolymers in aqueous media depend on copolymer composition profile

Barbara Farias-Mancilla [a], Arianna Balestri [b], Junliang Zhang [c,d], Henrich Frielinghaus [e], Debora Berti [b], Costanza Montis [b], Mathias Destarac [a], Ulrich S. Schubert [c,d], Carlos Guerrero-Sanchez [c,d,*], Simon Harrisson [f,*], Barbara Lonetti [a,*]

[a] Laboratoire Softmat, Université de Toulouse, CNRS UMR 5623, Université Toulouse III – Paul Sabatier, France
[b] Department of Chemistry "Ugo Schiff", University of Florence and CSGI, Florence, Italy
[c] Laboratory of Organic and Macromolecular Chemistry (IOMC), Friedrich Schiller University Jena, Jena, Germany
[d] Jena Center for Soft Matter (JCSM), Friedrich Schiller University Jena, Jena, Germany
[e] Forschungszentrum Jülich GmbH, Jülich Center for Neutron Science at Heinz Maier-Leibnitz Zentrum, Lichtenbergstrasse 1, 85747 Garching, Germany
[f] LCPO, CNRS/Bordeaux-INP/Université de Bordeaux, Pessac, France

GRAPHICAL ABSTRACT

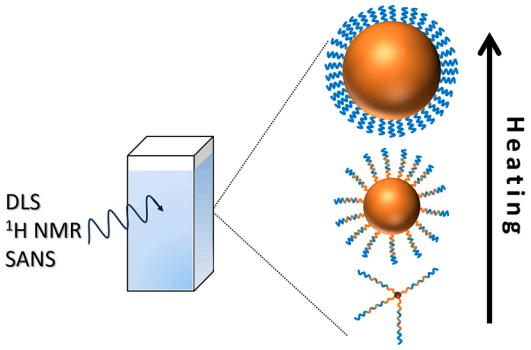

ARTICLE INFO

Keywords:
Thermoresponsive copolymers
Poly(*N*-isopropyl acrylamide) NIPAM
Poly(dimethyl acrylamide) PDMA
Gradient-like copolymers
Effect of composition profile
Self-assembly
SANS
NMR

ABSTRACT

Hypothesis: There is a lack of understanding of the interplay between the copolymer composition profile and thermal transition observed in aqueous solutions of *N*-isopropyl acrylamide (NIPAM) copolymers, as well as the correlation between this transition and the formation and structure of copolymer self-assemblies.
Experiments: For this purpose, we investigated the response of five copolymers with the same molar mass and chemical composition, but with different composition profile in aqueous solution against temperature. Using complementary analytical techniques, we probed structural properties at different length scales, from the molecular scale with Nuclear Magnetic Resonance (NMR) to the colloidal scale with Dynamic Light Scattering (DLS) and Small Angle Neutron Scattering (SANS).
Findings: NMR and SANS investigations strengthen each other and allow a clear picture of the change of copolymer solubility and related copolymer self-assembly as a function of temperature. At the molecular scale, dehydrating NIPAM units drag *N*,*N*-dimethyl acrylamide (DMA) moieties with them in a gradual collapse of the

* Corresponding authors.
E-mail addresses: carlos.guerrero.sanchez@uni-jena.de (C. Guerrero-Sanchez), simon.harrisson@enscbp.fr (S. Harrisson), barbara.lonetti@cnrs.fr (B. Lonetti).

https://doi.org/10.1016/j.jcis.2024.02.032
Received 13 October 2023; Received in revised form 18 January 2024; Accepted 4 February 2024
Available online 5 February 2024

copolymer chain; this induces a morphological transition of the self-assemblies from star-like nanostructures to crew-cut micelles. Interestingly, the transition spans a temperature range which depends on the monomer distribution profile in the copolymer chain, with the asymmetric triblock copolymer specimen revealing the broadest one. We show that the broad morphological transitions associated with gradient copolymers can be mimicked and even surpassed by the use of stepwise gradient (asymmetric) copolymers, which can be more easily and reproducibly synthesized than linear gradient copolymers.

1. Introduction

Thermoresponsive polymers such as poly(*N*-isopropyl acrylamide) (PNIPAM) have been studied for over 50 years [1]. PNIPAM is soluble in water up to ca. 32 °C; above this temperature, known as cloud point temperature, PNIPAM chains undergo dehydration, collapse and precipitate from aqueous solution. This lower critical solution temperature (LCST) behavior in a biological temperature range makes it an appealing stimuli-responsive system for biomedical applications. [2–4] In addition to PNIPAM, many other polymers, e. g., poly(propylene oxide) [5], polyacrylamides [1,6,7], polyoxazolines [8], poly(oligoethyleneglycol) acrylates [9], poly(*N*-vinyllactams) [10–12] and polypeptides [13,14], show similar LCST behavior provided that a right balance of hydrophilic and hydrophobic elements is in place. Most of the literature on thermoresponsive polymers concentrates on how the LCST can be increased or decreased via copolymerization with hydrophilic [15–17] or hydrophobic monomers, respectively [18,19]. For example, quaternization of only 3 mol% of the monomer units of poly(2-(dimethylamino)ethyl methacrylate) (PDMAEMA) leads to an increase in cloud point temperature from 28 to 61 °C [20]. Similarly, *N*-*n*-propyl acrylamide and *N*-ethyl acrylamide can be mixed in different amounts to modulate the cloud point temperature of their aqueous solutions from 20 to >85 °C [21]. Statistical or block copolymers of hydrophobic and hydrophilic monomers, such as ethyl lactate acrylate and *N*,*N*-dimethyl lactamide acrylate, may show LCST behavior even when their respective homopolymers do not [22].

Even the presence of low molar mass end groups in the polymer chains [23–27] or a change from linear to cyclic topology [28] can alter the LCST behavior. For example, the presence of a dodecyl end group lowers the cloud point temperature of PNIPAM [29], while the presence of a hydrophilic end group will increase it [7,29]. These effects decrease in intensity as the PNIPAM chain length increases. From the point of view of macromolecular design, this sensitivity to molecular architecture is both a blessing and a curse. On the one hand, thermoresponsive behavior can be modulated across a wide range of temperature; on the other hand, the combined or contrasting effect of these structural parameters must be considered when designing a thermoresponsive system, in particular if a control in the self-assembling properties is aimed.

Aqueous solutions of diblock copolymers containing a LCST segment and a hydrophilic segment undergo micellization upon heating, while triblock copolymers comprising two LCST blocks connected by a central hydrophilic block form gels if appropriately concentrated, or flowerlike micelles in a dilute regime [30–35]. In these cases, the hydrophilic segment must be sufficiently long to stabilize the formed micelles, but not so long as to inhibit interactions between the thermoresponsive segments. End groups can significantly affect the self-organization of the structures: the presence of a dodecyl group is sufficient to induce aggregation of PNIPAM and other thermoresponsive polyacrylamides at room temperature; [21,27,29,36] whereas with two dodecyl end groups, flower-like micelles can form [27]. A recent study of 3- and 5-block copolymers containing alternating segments of PNIPAM and hydrophilic poly(dimethyl acrylamide) (PDMA) with the same compositional ratio revealed that the way hydrophilic and hydrophobic segments are distributed along the chain modifies the aggregation behavior as a function of temperature [27]. In the case of the pentablock copolymer with a single dodecyl chain end, an anomalous cloud point behavior was observed by turbidimetry and it corresponded to the formation of stable mesoglobules at high temperatures.

Other examples in the literature show that even more complex interactions can be observed when polymer segments with different thermoresponsive behavior are combined, revealing the role of copolymer structure. A block copolymer formed of two statistical segments of *N*-propyl and *N*-ethyl acrylamide with individual cloud point temperatures of 37 and 52 °C, respectively, displayed a double transition as revealed by turbidimetry and dynamic light scattering (DLS) [21]. The transitions were broadened and displaced, with midpoints at 42 and 46 °C. Similarly, block statistical copolymers of *N*-acryloylpyrrolidine (APy, LCST = 47 °C) and *N*-acryloylpiperidine (APi, LCST = 4 °C) containing a P(APy) segment and a statistical segment of P(APy-*co*-APi) revealed two separate transitions when the difference in cloud point temperatures of the individual segments was greater than 20 °C, but a single broad transition when the difference was smaller [36].

Such broad transitions are frequently associated with gradient copolymers and are accompanied by modification of the self-assemblies in solution [37–40]. A thermoresponsive gradient copolymer can be regarded as a copolymer whose composition, and hence whose cloud point temperature, varies smoothly along the length of the chain. As temperature is increased, one would expect that an increasing fraction of the polymer will become insoluble. Indeed, aggregation of gradient copolymers of hydroxyethyl methacrylate and DMAEMA was detected by DLS around the cloud point temperature of their most hydrophobic end, while macroscopic clouding, corresponding to the formation of larger aggregates, was only observed at temperatures when around 30 % of the chain was estimated to be insoluble [40]. Gradient copolymers of vinyl ethers in water [39], and of lauryl methacrylate and styrene in a selective solvent for lauryl methacrylate [41] formed micelles that shrank as temperature was increased, which was attributed to a larger proportion of the polymer becoming insoluble and transferred from the swollen shell to the collapsed core.

This simple picture of gradient copolymers is appealing, but the examples of block and block-statistical copolymers cited above show that it is incomplete and a thorough understanding of the role of the copolymer microstructure is still missing. Aggregates of block-statistical copolymers of APy and APi also shrink as temperature is increased [36], while block copolymers of NIPAM and DMA [27], or ethyl lactate acrylate and dimethyl lactamide acrylate [22] can show similar behavior to statistical copolymers, their self-assemblies can grow in size or precipitate. Meanwhile, gradient copolymers may show the sharp transitions associated with statistical copolymers. [42,43].

Thus, the aim of this contribution is to explore the impact of the distribution of thermoresponsive monomer units along copolymer chains on thermal transitions and self-assembly in aqueous solution.

For this purpose, we synthesised five copolymers with a molar mass of 20 kg mol^{-1} and a global copolymer composition of 50 mol % DMA and 50 mol % NIPAM (Fig. 1): a P(NIPAM-*stat*-DMA) statistical copolymer (S20K), a PNIPAM-*block*-PDMA block copolymer (B20K), an asymmetric diblock copolymer with two P(NIPAM-*stat*-DMA) blocks with equal targeted molar mass of 10 kg mol^{-1} containing 84 mol % and 16 mol % NIPAM respectively (D20k), an asymmetric triblock with a short PNIPAM block, a P(NIPAM-*stat*-DMA) statistical segment containing 50 % NIPAM as well as a short PDMA block (T20K), and a P(NIPAM-*grad*-DMA) linear gradient copolymer (G20K). DMA was chosen because its homopolymer is soluble in water at all temperatures and it has a similar reactivity to NIPAM (r_{DMA} = 0.8, r_{NIPAM} = 1.1) [44]

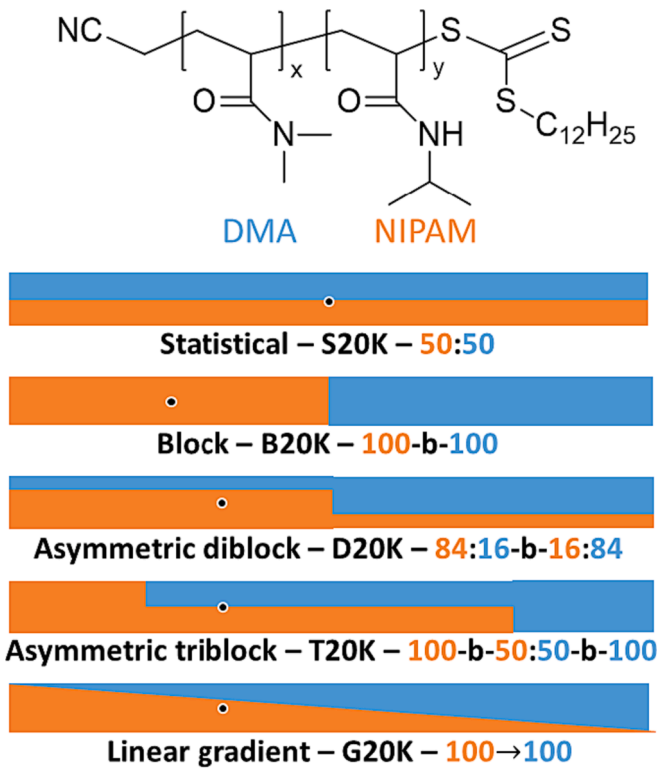

Fig. 1. Schematic representations of the chemical formula and of the investigated NIPAM-DMA copolymer composition profiles. The orange fraction represents the proportion of NIPAM in the copolymer along the chain: for example, it is constant in the statistical copolymer in which NIPAM is randomly mixed with DMA; it varies gradually from one end, mainly composed of NIPAM, to the other, mainly composed of DMA, in the case of linear gradient copolymer. The center of mass of the distribution of NIPAM monomer units within the copolymer is represented by a black dot (see SI for more details). (For interpretation of the references to colour in this figure legend, the reader is referred to the web version of this article.)

allowing the formation of near random copolymers across a wide range of feed compositions with minimal composition drift.

The same overall composition was chosen for all copolymers so that changes in the assembly behaviour could not be attributed to differences in the content of the hydrophilic monomer and its influence on the cloud point value or on the hydrophobic/hydrophilic ratio above NIPAM transition. The composition profiles of the G20K, D20K and T20K copolymers were selected so that the expected value of the position of the center of mass of the NIPAM units is 0.33 of the total length of the polymer chain, measuring from the NIPAM-rich end. For comparison, the corresponding values for the block and statistical copolymers are 0.25 and 0.5, respectively (see Supporting Information, SI, section S1.3 for details).

We examined copolymer aqueous solutions over a temperature range from room temperature to 70 °C, well above the NIPAM cloud point temperature. To unravel the molecular details of the NIPAM thermal transition and its impact on copolymer self-assembly on a range of length scales—from molecular to hundreds of nanometers—we employed DLS, proton nuclear magnetic resonance (^{1}H NMR), and small-angle neutron scattering (SANS) techniques.

2. Materials and methods

2.1. Synthetic procedures

(Co)polymerizations of DMA and NIPAM were conducted via the reversible addition-fragmentation chain transfer (RAFT) process. The gradient profile was obtained with a starved feed semi-batch process. The asymmetric diblock and triblock copolymers were synthesized using a robotic parallel synthesizer. See SI section S1 for details.

2.2. Dynamic light scattering (DLS)

DLS experiments were performed on a Malvern Zetasizer Nano ZS equipped with a 633 nm laser module and a detection angle of 173°. Measurements were triplicated; each one with a duration of 300 s. Solutions of 1 wt% of copolymer were prepared in ultrapure water and temperature was varied between 25 and 70 °C using 5 °C steps.

2.3. Proton nuclear magnetic resonance(^{1}H NMR) at different temperatures

^{1}H NMR experiments as a function of temperature (from 25 °C up to 70 °C with 5 °C intervals) were performed on a Bruker Avance III HD 400 MHz spectrometer equipped with a 5 mm TBO probe. The used measuring parameters were: Pulse sequence zgpr (program with pre saturation of the water signal), number of accumulation (NS = 32), relaxation time (D1 = 2 s), acquisition time (AQ = 4 s) and temperature range from 298 to 343 K. All the copolymer solutions were prepared in deuterium oxide (D_2O) at a concentration of 1 wt%. 3(trimethylsilyl)-propionic acid-D_4 (10 mM) was used as chemical shift internal reference (0 ppm) and as internal standard. To estimate the ratio of NIPAM to DMA units in aqueous solution, the integral values of the corresponding signals were utilized in the following normalized equations:

$$r_{NIPAM,w} = \frac{\int NIPAM}{(\int NIPAM + \int DMA)}; r_{DMA,w} = \frac{\int DMA}{(\int NIPAM + \int DMA)} \quad (1)$$

The change in the obtained integral values as a function of temperature was then fit to a sigmoidal error function (equation (2) using a nonlinear least squares fitting.

$$A = \frac{A_0 + A_f}{2} - \frac{A_0 - A_f}{2}\,\mathrm{erf}\left(\frac{T - T_{½}}{\sqrt{2}\,\sigma}\right) \quad (2)$$

In this model, A_o represents the integral value of the signal at low temperature, A_f the integral value of the signal at high temperature, $T_{½}$ the temperature midpoint of the transition, and σ is a parameter that determines the width of the transition (68 % of the transition takes place between $T_{½}$-σ and $T_{½}$+σ). More details and all the results obtained from this procedure are shown in Figure S10, and the corresponding parameters are summarized in Tables 1 and S7 in SI.

2.4. Small angle Neutron scattering (SANS)

SANS measurements were performed on KWS-1 at the research reactor FRM II (Jülich Centre for Neutron Science) [45]. All samples were measured at the following settings: 8/1.13/4.93, 8/7.63/4.93, with collimation and detector distances in m, and wavelength in Å. This led to a q-range from 0.007 to 0.4 $Å^{-1}$. All data were corrected for background and detector efficiency, radially averaged and calibrated to absolute units (with a secondary plexiglass sample) using the software qtiKWS and qtiSAS (https://www.qtisas.com). The acquisition times were chosen so that the radially averaged intensities had a statistical noise lesser than 1 %. The temperature of the 2x12 sample rack was controlled using a recirculating water bath.

The data were interpreted using two different models with the SASfit program. One model was developed by Dozier for star polymers where the polymer branches come out from the centre forming blobs [46]. It is composed of a Guinier term to determine the gyration radius of the nano-object and a mass fractal term for the contribution of the polymer arms.

The other selected model describes micelles with a homogeneous core and a shell with a decaying density profile. The chains in the shell

are semi flexible with excluded volume effects. For a detailed description of the data modelling, we refer the reader to SI section S4.

3. Results and discussion

We first performed DLS measurements on the five copolymers of different composition profile at temperatures ranging from 25 to 70 °C using 5 °C increments. All hydrodynamic diameters (D_h) and polydispersity index (PDI) values are summarized in Table S6 and Figures S6-S8 in SI; some of them are reported in Fig. 2.

The copolymers of this study self-assemble below the LCST of PNIPAM because of the presence of the hydrophobic dodecyl group of the RAFT agent (see chemical structure in Fig. 1), as has previously been reported [29] for PNIPAM homopolymers in the molar mass range from 1 to 11 KDa. At 25 °C all copolymers, except G20K, show a monomodal distribution of assemblies with a PDI value lower than 0.2 and particle size in the range from 22 to 25 nm.

The G20K particle assemblies display a bimodal intensity-weighted distribution, with a major component having a size similar to the other investigated copolymers (around 30 nm) and a minor component in the 200 nm range, possibly due to some ill-defined aggregates (refer to Fig. 2a and b and SI, Figure S8). As the intensity-weighted distribution is strongly biased towards larger particles, the minor component represents a negligible fraction of the mass and number distributions.

Upon heating, all copolymer self-assemblies, except the S20K, increased in size and decreased in PDI value (see Fig. 2c). They revealed a broad transition starting around 30 °C and reaching a plateau around 50 to 60 °C, depending on the copolymer composition profile. No precipitation was observed under the investigated experimental conditions, which suggests that the self-assemblies were stabilized by the PDMA-rich segments in the copolymer chains that conveyed dispersibility to the nanostructures even at relatively high temperatures. By contrast, the statistical copolymer S20K did not significantly change in size up to 55 °C, and precipitated at 60 °C (Figure S6 and Table S6 in SI) in agreement with previous reports [15].

To better understand the phase transition of the investigated copolymers at the molecular level, ^{1}H NMR investigations of aqueous solutions of the copolymers (10 mg mL^{-1} in D_2O) in the temperature range from 25 to 70 °C [38,47] were performed (Figure S9 in SI displays typical ^{1}H NMR spectra obtained from these investigations).

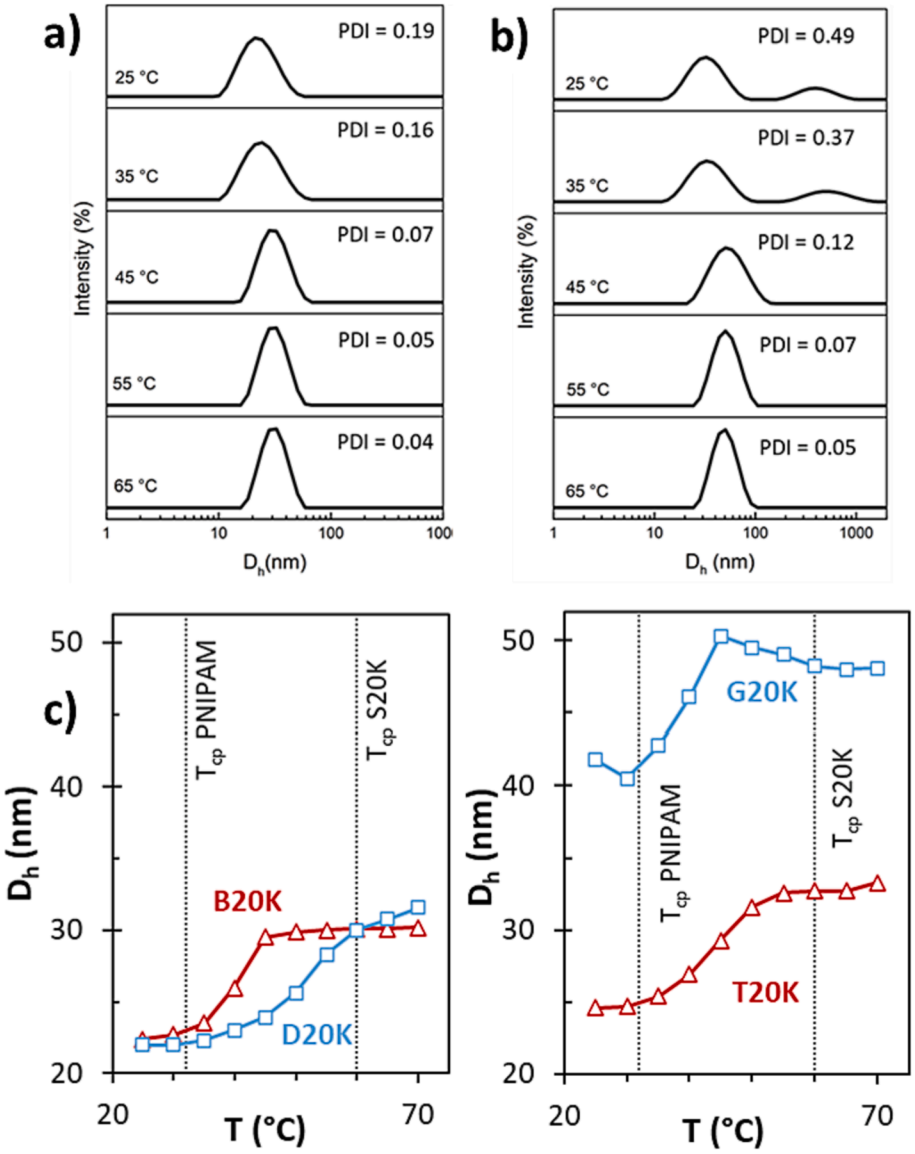

Fig. 2. Intensity weighted size distributions of hydrodynamic diameters measured by DLS at different temperatures for B20K (a) and G20K (b); c) Z-average hydrodynamic diameters as a function of temperature for all copolymers. Dashed lines at 32 °C and 60 °C correspond to the cloud point temperature of PNIPAM and 1:1 P(NIPAM-*co*-DMA) statistical copolymer, respectively.

These ^{1}H NMR measurements enabled us to distinguish changes in the solubility of each type of monomer as a function of temperature as the evolution of the signals of the methylene proton of NIPAM at 3.9 ppm and the methyl proton of DMA at 3 ppm can be regarded as local markers of chain collapse. As shown in Fig. 3 for the case of G20K (and Figure S10 in SI for all the copolymers), upon heating, the integral value of the ^{1}H NMR signals ascribed to NIPAM and DMA units decreased, indicating restricted motion of monomer segments as the polymer chains collapse; this has previously been observed for NIPAM signals for example [38,47] and can be used to determine the midpoint of polymer collapse in an analogous way to the critical micellar temperature as already shown for Pluronics [48,49]. Interestingly, we found that the integral value of these NIPAM and DMA signals decreased at rates that varied according to the compositional profiles of the copolymers.

The results are consistent with a polymer collapse that originates at the dodecyl end group and gradually moves along the polymer chain as shown by the agreement between the experimental NMR data and the model shown in Fig. 3 (see Figure S11 and section S3 in SI for details). Hence, in the case of B20K, the integral value of the ^{1}H NMR signals ascribed to the NIPAM units decreased, while those of the DMA units remained nearly constant. For the copolymers D20K, T20K and G20K, by contrast, the integral value of the ^{1}H NMR signals of both NIPAM and DMA units decreased in a manner that was consistent with their changing composition profiles. This is particularly evident for the gradient copolymer G20K, whose changing ^{1}H NMR signals are consistent with the increase in the DMA content of the collapsing polymer (Fig. 3 – G20K; results for all the investigated copolymers can be found in Figure S11 in SI).

The apparent NIPAM:DMA ratio in D_2O at 25 °C, was typically lower than the ratio determined in $CDCl_3$, a good solvent for both segments (Table S7 in SI) which, in turn, was consistent with the expected ratio, based on the conversion of each monomer during copolymer synthesis. This indicates that even at room temperature the NIPAM-rich segments are partially collapsed, which is consistent with the aggregates observed with DLS.

The ^{1}H NMR results were used to determine the fraction of collapsed polymer as a function of temperature, as shown in Fig. 4. Regardless of the composition profile of the investigated copolymers, heating from 25 to 70 °C results in a collapse of ca. 40 to 50 % of the monomer units in the copolymer chains. For the block and asymmetric diblock copolymers (B20K and D20K, respectively), this corresponds to ca. 80 % of the NIPAM-rich segment, while for the triblock copolymer this corresponds to the entire NIPAM homopolymer block and up to half of the 1:1 DMA:NIPAM copolymer block.

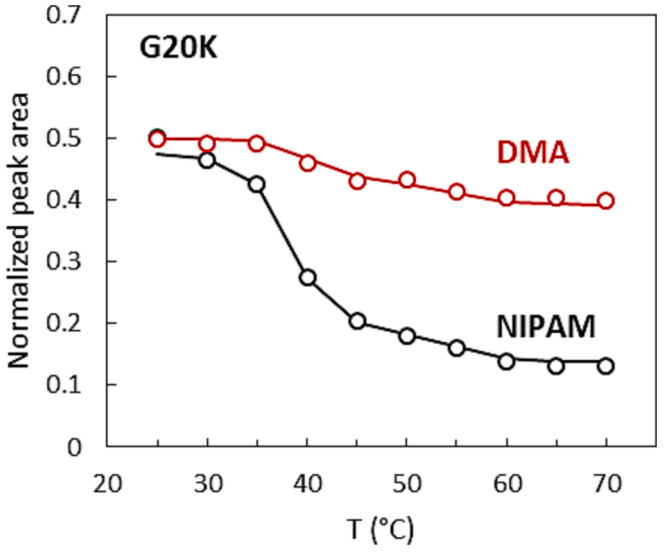

Fig. 3. Progressive polymer chain collapse in aqueous solution as a function of temperature for copolymer G20K. Red and black circles show the normalized integral value of the ^{1}H NMR signals for DMA and NIPAM, respectively. Red and black lines show the predicted normalized integral value of the ^{1}H NMR signals for the corresponding fraction of collapsed polymer based on the copolymer composition profile (see section S3 in SI for details). (For interpretation of the references to colour in this figure legend, the reader is referred to the web version of this article.)

The increase in the fraction of collapsed polymer chains with increasing temperature was empirically fitted to a 4-parameter sigmoidal function (see SI for details of the fitting procedure). This function was used to establish the midpoint of the thermal transition ($T_{½}$), as well as a parameter related to its breadth (2σ). These parameters are summarized in Table 1.

As temperature increased, the chain collapse was first observed for the block copolymer B20K (around 35 °C), followed by the gradient copolymer G20K (around 40 °C) and, finally, for the asymmetric diblock copolymer D20K (around 45 °C). The thermal transition corresponding to B20K is sharper (2σ = 9 °C) than that of the gradient (2σ = 13 °C) and asymmetric diblock (2σ = 14 °C) copolymers. Finally, the asymmetric triblock copolymer T20K displayed a considerably broader transition (2σ = 24 °C) centred around 41 °C. Although this copolymer contains two thermoresponsive segments, only a single, very broad, thermal transition was detected. For comparison, polymers with the same composition as the triblock segments, PNIPAM homopolymer and 1:1 P(DMA:NIPAM) statistical copolymer, precipitated abruptly at 32 °C and 60 °C, respectively.

These results show that chain collapse in both the block and gradient copolymers takes place across a wide temperature range, even for block copolymers with a sharp or a step-wise change in composition. The presence of a hydrophilic block increases both the midpoint and breadth of the thermal transition, suggesting an effect which is strongest at the junction of the two blocks, and diminishes as the distance from the junction increases. As a result, the asymmetric triblock copolymer T20K yields a thermal transition even broader than that of its analogous linear gradient copolymer.

We further evaluated the effects of temperature and composition profile on the structure of the self-assembled copolymers using SANS and connected the described ^{1}H NMR findings with the SANS results. Scattering curves were recorded at 5 different temperatures in the range from 25 to 65 °C (Figs. 5 and 6). All fitting parameters are reported in Tables S8 to S11 in SI, while the most relevant ones are summarized in Table 2.

At 25 °C, well below $T_{1/2}$, the scattering curves of all the investigated copolymers (shown in Fig. 5a and Figure S16) reveal the presence of self-assembled nanostructures, in accordance with the DLS and NMR results. This self-assembly process is driven by hydrophobic interactions between the dodecyl end groups of the copolymer chains.

The observed scattering patterns resemble those typically observed for star-like polymers, which are well described by the Dozier model (see black lines in Fig. 5a and details in SI) [50]: they exhibited a Guinier region at low q values followed by a power-law trend in the high q range: $I(q) \sim q^{(-1/\nu)}$, where ν represents the Flory exponent which depends on the quality of the solvent. For all copolymer solutions, the Flory exponent is equal to 1.6, suggesting that the polymer chains are swollen in solution. The Dozier model distinguishes two main length scales: the radius of gyration, R_g, of the self-assembly and the correlation length, ξ, inside the star. [46] From SANS analysis of the data at 25 °C, we conclude that all of the copolymers form star-like assemblies with a low aggregation number (in the range from 3 to 7) and a radius of gyration in the range from 81 to 93 Å (see Table 2). At this temperature, the observed differences in size can be ascribed to differences in the molar mass of the copolymer chains, without a significant effect of the copolymer composition profile.

The scattering curves recorded at 65 °C, well above $T_{1/2}$, are displayed in Fig. 5b (Figure S16 at 55 °C before precipitation for S20K). At this temperature, the thermal transition detected by NMR is complete.

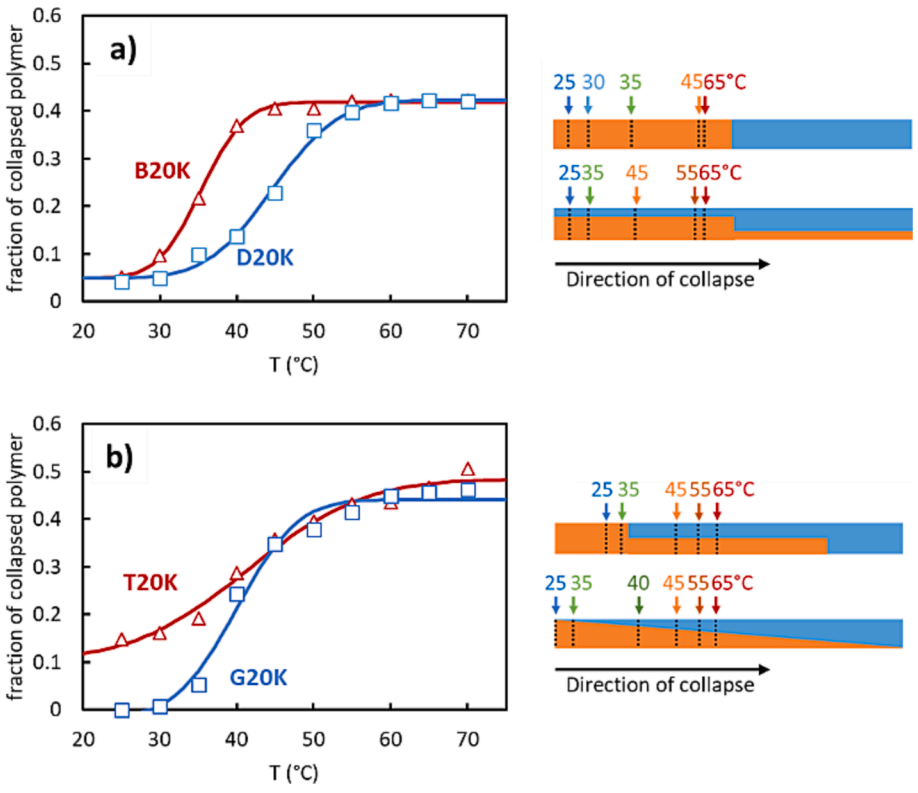

Fig. 4. Fraction of collapsed polymer (assuming a progressive chain collapse from the $C_{12}H_{25}$ terminus) as a function of temperature for the investigated copolymers: a) B20K and D20K; b) T20K and G20K. Open symbols represent experimental points derived from NMR measurements, while the solid curves represent the best fit of a 4-parameter sigmoidal function used to establish the location and breadth of the thermal transition. On the right side of both plots, there is a schematic representation of the fraction of collapsed polymer at different temperatures.

Table 1
Characteristic values of the thermal transition of copolymer aqueous solutions. $T_{1/2}$ corresponds to the midpoint of the transition, while 2σ is an indication of its breadth. The values were obtained by fitting experimentally obtained integral values of ^{1}H NMR signals (A) to equation (2). $X_{INITIAL}$ and X_{FINAL} correspond to the fraction of collapsed polymer at low and high temperature, respectively, and were obtained using equation S2 – S6 in SI. *The apparent negative value of $X_{INITIAL}$ for G20K can be attributed to uncertainty in the integration procedure of the corresponding NMR signals and is not significantly different from zero.

	$T_{1/2}$ (°C)	2σ (°C)	$X_{initial}$	X_{FINAL}
B20K	35	9	0.05	0.42
D20K	45	14	0.05	0.42
T20K	41	24	0.11	0.47
G20K	40	13	−0.02*	0.44

For all copolymers, except S20K, the shape of the curves changes considerably with respect to T = 25 °C:

(i) The power-law trend appears at higher q values, while the Flory exponent approaches 1, characteristic of polymer chains in a semi-dilute regime. This indicates an obvious change in the solvent quality at T = 65 °C due to the presence of NIPAM in the copolymer chain.

(ii) In the intermediate q range, a significant change in the slope of the curves and an oscillation are observed, which suggests the formation of core–shell micelles.

(iii) Furthermore, the scattering intensity at low q values increases, which indicates an increase in the aggregation number of the self-assemblies. This can be ascribed to the greater hydrophobicity of NIPAM-rich segments when heated above their cloud point temperature, which promotes polymer–polymer interactions.

All these curves are well described by a model that includes a homogeneous core formed by the collapsed polymer fraction obtained by NMR and a shell with a decaying density profile. The contribution of polymer segments in the shell is described by semi-flexible chains with excluded volume effects (see section S4 in SI for details).

From the results reported in Table 2, we conclude that when the NIPAM transition is complete, the copolymer self-assemblies are crew-cut micelles, with a core radius greater than the thickness of the shell (see Table 2). The total radius (core + shell) of the micelles is within 10 % of the hydrodynamic radius measured by DLS, indicating the good agreement between the results of the different experimental techniques. The polymer chains in the core are highly stretched and hydrated with a fraction of solvent ranging from 0.66 to 0.73, similar to the meso-globules formed by multiblock P(NIPAM-DMA) copolymers observed by Ohnsorg et al. [27] This may explain why the NMR signals attributed to NIPAM protons do not completely vanish at high temperature, even in the block copolymer B20K.

Any small differences in size between the different comonomer composition profiles (i.e, block, diblock and triblock copolymers) are within the uncertainty of the fitting procedure of the experimental results (see Table 2). Hence, it can be concluded that the comonomer composition profile does not significantly impact the behaviour of these systems at temperatures well above (65 °C) or below (25 °C) the thermal transition, and that the structural details of the self-assemblies are mainly determined by the overall hydrophobic fraction (related to the fraction of collapsed polymer chains in Fig. 4 and Table 1, which is ca. 0.4 for all copolymers).

Nevertheless, S20K, where NIPAM and DMA monomer units are randomly mixed, behaves differently. Its SANS curve was not sensibly affected by temperature: only a contraction of the core of the assemblies was observed (the scattering curve moves to smaller q values) and some aggregation phenomena before precipitation was observed at higher temperature (a slight increase of the low q scattering intensity), which confirms what was observed by DLS (see Figure S16). This difference

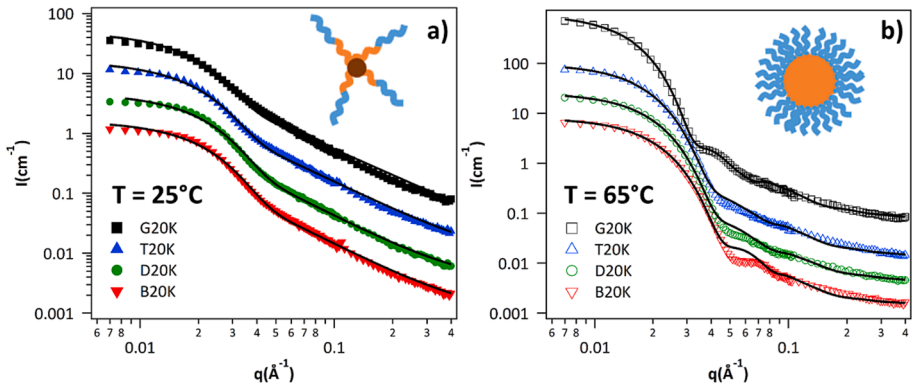

Fig. 5. Neutron scattering intensity as a function of the scattering vector for the different copolymers with molar mass of 20 kDa at a) T = 25 °C and b) T = 65°; the curves have been arbitrarily shifted to facilitate comparisons. The black solid lines are the fitted curves using the Dozier model at T = 25 °C and core–shell model (homogeneous core and decaying density profile in the shell) at T = 65 °C.

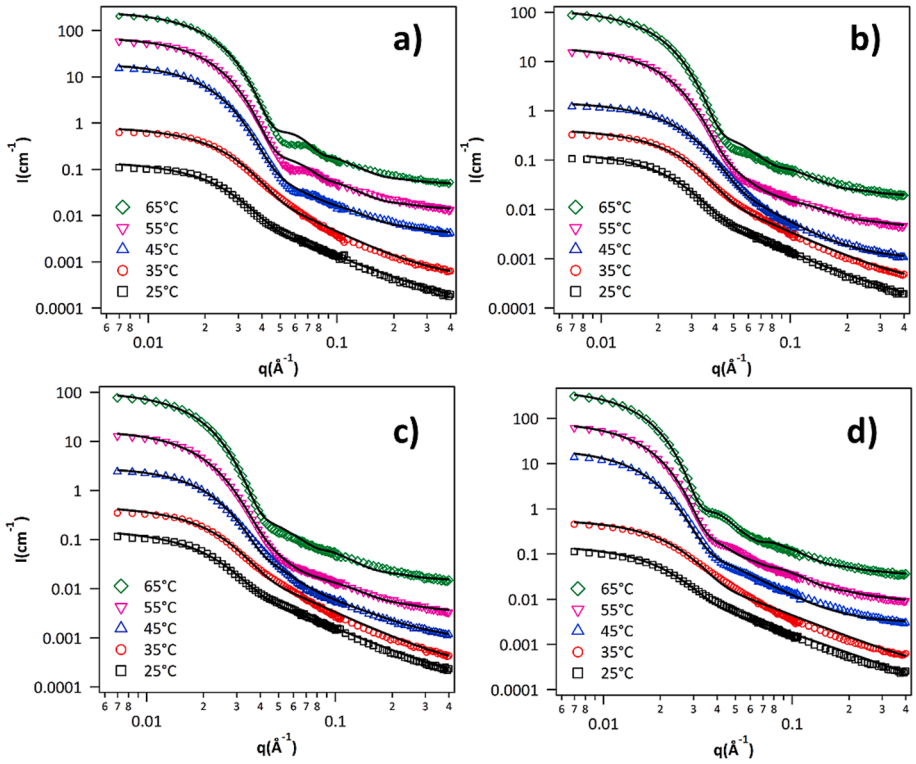

Fig. 6. Neutron scattering intensity as a function of the scattering vector at temperatures between T = 35 °C and T = 65 °C for the different copolymers with molar mass 20KDa; a) B20k, b) D20k, c) T20k and d) G20k. The curves have been arbitrarily shifted to allow a better comparison. The black solid lines are the best fits using the models described in the text.

indicates the need for a DMA polymer sequence long enough to stabilize the self-assemblies and confirms the role of thermoresponsive monomer distribution in the control of the morphological transition.

However, the behaviour of these systems is significantly different around their transition. The structural changes that occur between 25 and 65 °C depend on the comonomer composition profile. The scattering curves recorded at different temperatures (see Fig. 6) reveal details of the evolution from star-like self-assemblies to crew-cut micelles.

The morphological evolution of self-assemblies of block copolymer B20K (Fig. 6a) is mainly ascribed to the collapse of the NIPAM segments as characterized by ^{1}H NMR. At 35 °C, the thermal transition is at its onset and the self-assemblies are still well described by a star-like polymer model. At this temperature, changes in the curves mainly occur in the low q region, which relates to the overall size of the nanostructures. The aggregation number is slightly increased as compared to 25 °C, suggesting that dehydration of the NIPAM units is the main driving force for the structural changes.

At 45 °C, the transition towards crew-cut micelles is practically complete. The scattering curve shows the oscillations typically observed in spherical core–shell micelles. No further significant changes are observed upon heating the system above 45 °C, in agreement with the NMR measurements (Fig. 4a).

The scattering curves of aqueous solutions of copolymer G20K are displayed in Fig. 6d. Here too, the morphological transition to crew-cut micelles is complete at 45 °C. In this case, however, the micelles continue to evolve upon further heating, with an increase in the core radius and aggregation number, and a slight decrease in the shell thickness. This is consistent with NMR measurements showing that the fraction of collapsed chains slowly increases from 0.35 at 45 °C to 0.46 at 65 °C (Fig. 4b). Both NIPAM and DMA units are involved in the chain

Table 2
Values of the fitting parameters obtained from the Dozier and micelle models. R_g is the overall radius of gyration of the self-assemblies; N_{ag} is the aggregation number; R_{core} is the radius of the core; t_{shell} is the thickness of the shell.

B20k	25 °C	35 °C	45 °C	55 °C	65 °C	G20k	25 °C	35 °C	45 °C	55 °C	65 °C
R_g (Å)	81[a]	80[a]	96[b]	96[b]	97[b]		93	87	125	131	142
N_{ag} [c]	4	6	26	31	33		3	5	36	55	75
R_{core} (Å)[d]			79 ± 15	86 ± 13	90 ± 12				84 ± 18	105 ± 15	117 ± 14
t_{shell} (Å)[d]			48 ± 1	50 ± 1	49 ± 1				65 ± 14	59 ± 7	59 ± 7
N_{ag}^d			32	44	50				42	80	124
D20k						**T20k**					
R_g (Å)	82 [a]	76 [a]	75 [a]	96[b]	103[b]		89 [a]	85 [a]	96 [a]	105[b]	112[b]
N_{ag} [c]	4	5	9	28	40		3	4	13	24	35
R_{core} (Å)[d]			44 ± 8	77 ± 15	91 ± 13				61 ± 14	78 ± 17	96 ± 14
t_{shell} (Å)[d]			63 ± 7	42 ± 5	44 ± 5				55 ± 18	48 ± 9	54 ± 9
N_{ag}^d			13	38	62				15	31	57

a) obtained from Dozier model; b) obtained from Guinier fit; c) obtained from low q absolute intensity values; d) obtained from micelle fitting.

collapse. The pronounced increase in aggregation number from 45 to 65 °C indicates that micelles continue to grow, either by fusion or by individual transfer of polymer chains via an Ostwald ripening-type process.

For copolymers D20K and T20K, the morphological transition occurs more gradually (see Fig. 6b and 6c). Upon heating from 25 to 35 °C, the aggregation number slightly increases with a negligible effect on the radius of gyration of the nanostructures. The structures are well described by the Dozier model, indicating a star-like polymer structure. At 45 °C both star-like polymer and crew-cut micelle models adequately describe the data. This may indicate the co-existence of both types of self-assemblies and/or an intermediate structure between a star-like polymer and crew-cut micelles.

At 55 °C the transition to crew-cut micelles is complete for both D20K and T20K samples, and the Dozier model no longer adequately describes the scattering data. The core radius and aggregation number continue to increase as temperature increases from 55 to 65 °C, while the shell thickness slightly decreases (D20K) or remains roughly constant (T20K). Broadly speaking, the comparisons of aggregation numbers with the core radius align with the findings from NMR studies, indicating a propensity for the collapse of polymer chains along the transition. The shell thickness parameter is somewhat more nuanced, yet it also indicates subtle tendencies toward collapse.

Thus, the morphological transitions of these self-assembled nanostructures are impacted by the copolymer composition profile, despite their identical overall compositions. The thermal transition of copolymer B20K, containing only homopolymer blocks, is complete at 45 °C and little structural change is observed upon further heating. On the other hand the asymmetric diblock, triblock and gradient copolymers D20K, T20K, and G20K form self-assemblies that continue to evolve even after the morphological transition from star-like polymer to crew-cut micelle structures is complete, increasing in both size and aggregation number as the collapse of the copolymer chains continues upon further heating.

4. Conclusions

Our results demonstrate that by an appropriate design of the copolymer composition profile, keeping the same overall chemical composition, it is possible to modulate both the location and breadth of the thermal transition, which can be even broader than those that can be obtained from linear gradient copolymers. In particular, we show that:

(i) the thermal transitions have a subtle influence on the self-assembling properties which can then be tailored by adjusting the monomer profile in copolymer chains with the same chemical composition.

The presence of opportunely distributed hydrophilic monomers in a NIPAM-based copolymer not only influences its transition temperature in aqueous solution, but also increases the breadth of the transition. At the molecular scale, dehydrating NIPAM units drag DMA monomer units with them in a gradual collapse of the copolymer chain. This collapse starts from the hydrophobic end group and propagates along the chain towards the hydrophilic end. The gradual collapse of NIPAM-rich segments does not induce polymer precipitation, due to the presence of hydrophilic DMA-rich segments, but it causes a morphological transition of the self-assemblies from star-like polymer to crew-cut micelles.

(ii) the transition spans a temperature range which depends on the monomer distribution profile in the copolymer chain. An asymmetric diblock copolymer composed of two statistical blocks with different mean compositions shows a transition of similar breadth to that of a gradient copolymer, although at a slightly higher temperature, while an asymmetric triblock copolymer shows an even broader transition.

(iii) gradient-like behaviour can be obtained from block copolymers containing only two or three statistical segments, which are obtained by a much simpler synthetic procedure than that required for gradient copolymers.

The use of complementary techniques, DLS, NMR, and SANS, which probe scales ranging from molecular to *meso*-scale, is essential for an in-depth characterization of structural transitions of thermoresponsive copolymers with block, gradient and asymmetric block-statistical copolymer profiles.

In particular, the results of NMR analysis were used in an original way to refine the interpretation of data obtained from SANS, leading to a clearer picture of the chain collapse process than that could be obtained from either technique in isolation.

In summary, these results demonstrate the use of macromolecular engineering to generate materials which gradually transition from one to another state and open new avenues for the preparation of nanoparticles with continuous and nuanced responses to changes in their environment, a prerequisite of truly smart materials.

CRediT authorship contribution statement

Barbara Farias-Mancilla: Conceptualization, Formal analysis, Methodology, Writing – original draft, Writing – review & editing. **Arianna Balestri:** Data curation, Formal analysis. **Junliang Zhang:** Investigation, Writing – review & editing. **Henrich Frielinghaus:** Investigation, Writing – review & editing. **Debora Berti:** Writing – review & editing. **Costanza Montis:** Writing – review & editing. **Mathias Destarac:** Writing – review & editing. **Ulrich S. Schubert:** Writing – review & editing. **Carlos Guerrero-Sanchez:** Funding acquisition, Supervision, Writing – review & editing. **Simon Harrisson:** Funding acquisition, Supervision, Writing – original draft, Writing – review & editing, Formal analysis. **Barbara Lonetti:** Conceptualization, Formal analysis, Methodology, Writing – original draft, Writing – review & editing.

Declaration of competing interest

The authors declare that they have no known competing financial

interests or personal relationships that could have appeared to influence the work reported in this paper.

Data availability

Data will be made available on request.

Acknowledgements

This research was financially supported by the ASYMCOPO Project, an international collaborative research project of the Deutsche Forschungsgemeinschaft (DFG, Germany) and the Agence Nationale de la Recherche (ANR, France); DFG project: GU 1685/1-1 (J.Z., U.S.S and C. G-S.) and ANR project: ANR-15-CE08-0039 (S.H.). C.G-S. and U.S.S. thank the Collaborative Research Center "PolyTarget" (SFB 1278, (project number 316213987), projects B02 and Z01) of the DFG for financial support. This work is based upon experiments performed at the KWS-1instrument operated by Forschungszentrum Jülich GmbHat the Heinz Maier-Leibnitz Zentrum (MLZ), Garching, Germany. All authors thank Dr Joachim Kohlbrecher for modifying the program code of SASFit to adapt the model we used to our needs.

Appendix A. Supplementary material

Supplementary data to this article can be found online at https://doi.org/10.1016/j.jcis.2024.02.032.

References

[1] A. Halperin, M. Kröger, F.M. Winnik, Poly(N-isopropylacrylamide) Phase Diagrams: Fifty Years of Research, Angew. Chem. Int. Ed. 54 (2015) 15342–15367, https://doi.org/10.1002/anie.201506663.
[2] D. Roy, J.N. Cambre, B.S. Sumerlin, Future perspectives and recent advances in stimuli-responsive materials, Prog. Polym. Sci. 35 (2010) 278–301, https://doi.org/10.1016/j.progpolymsci.2009.10.008.
[3] J. Hoffman, W. Phillip, 100th Anniversary of Macromolecular Science Viewpoint: Integrated Membrane Systems, ACS MACRO Lett. 9 (2020) 1267–1279, https://doi.org/10.1021/acsmacrolett.0c00482.
[4] H. Cabral, K. Miyata, K. Osada, K. Kataoka, Block Copolymer Micelles in Nanomedicine Applications, Chem. Rev. 118 (2018) 6844–6892, https://doi.org/10.1021/acs.chemrev.8b00199.
[5] K. Mortensen, J.S. Pedersen, Structural study on the micelle formation of poly (ethylene oxide)-poly(propylene oxide)-poly(ethylene oxide) triblock copolymer in aqueous solution, Macromolecules 26 (1993) 805–812, https://doi.org/10.1021/ma00056a035.
[6] K. Kolouchová, V. Lobaz, H. Beneš, V.R. de la Rosa, D. Babuka, P. Švec, P. Černoch, M. Hrubý, R. Hoogenboom, P. Štěpánek, O. Groborz, Thermoresponsive properties of polyacrylamides in physiological solutions, Polym. Chem. 12 (2021) 5077–5084, https://doi.org/10.1039/D1PY00843A.
[7] F. Yin, P. Laborie, B. Lonetti, S. Gineste, Y. Coppel, N. Lauth-de Viguerie, J.-D. Marty, Dual Thermo- and pH-Responsive Block Copolymer of Poly(N-isopropylacrylamide)-block-Poly(N, N-diethylamino Ethyl Acrylamide): Synthesis, Characterization, Phase Transition, and Self-Assembly Behavior in Aqueous Solution, Macromolecules 56 (2023) 3703–3720, https://doi.org/10.1021/acs.macromol.3c00424.
[8] R. Hoogenboom, H. Schlaad, Thermoresponsive poly(2-oxazoline)s, polypeptoids, and polypeptides, Polym. Chem. 8 (2016) 24–40, https://doi.org/10.1039/C6PY01320A.
[9] G. Vancoillie, D. Frank, R. Hoogenboom, Thermoresponsive poly(oligo ethylene glycol acrylates), Prog. Polym. Sci. 39 (2014) 1074–1095, https://doi.org/10.1016/j.progpolymsci.2014.02.005.
[10] L. Etchenausia, A.M. Rodrigues, S. Harrisson, E. Deniau Lejeune, M. Save, RAFT Copolymerization of Vinyl Acetate and N-Vinylcaprolactam: Kinetics, Control, Copolymer Composition, and Thermoresponsive Self-Assembly, Macromolecules 49 (2016) 6799–6809, https://doi.org/10.1021/acs.macromol.6b01451.
[11] H. Peng, K. Rübsam, C. Hu, F. Jakob, U. Schwaneberg, A. Pich, Stimuli-Responsive Poly(N-Vinyllactams) with Glycidyl Side Groups: Synthesis, Characterization, and Conjugation with Enzymes, Biomacromolecules 20 (2019) 992–1006, https://doi.org/10.1021/acs.biomac.8b01608.
[12] X. Zhao, O. Coutelier, H.H. Nguyen, C. Delmas, M. Destarac, J.-D. Marty, Effect of copolymer composition of RAFT/MADIX-derived N-vinylcaprolactam/N-vinylpyrrolidone statistical copolymers on their thermoresponsive behavior and hydrogel properties, Polym. Chem. 6 (2015) 5233–5243, https://doi.org/10.1039/C5PY00606F.
[13] E. Garanger, S. Lecommandoux, Emerging opportunities in bioconjugates of Elastin-like polypeptides with synthetic or natural polymers, Adv. Drug Deliv. Rev. 191 (2022) 114589, https://doi.org/10.1016/j.addr.2022.114589.
[14] M. Badreldin, R. Le Scouarnec, S. Lecommandoux, S. Harrisson, C. Bonduelle, Memory Effect in Thermoresponsive Proline-based Polymers, Angew. Chem. Int. Ed. 61 (2022) e202209530.
[15] I.C. Barker, J.M.G. Cowie, T.N. Huckerby, D.A. Shaw, I. Soutar, L. Swanson, Studies of the "Smart" Thermoresponsive Behavior of Copolymers of N-Isopropylacrylamide and N, N-Dimethylacrylamide in Dilute Aqueous Solution, Macromolecules 36 (2003) 7765–7770, https://doi.org/10.1021/ma034250m.
[16] Y. Zhou, K. Jiang, Q. Song, S. Liu, Thermo-Induced Formation of Unimolecular and Multimolecular Micelles from Novel Double Hydrophilic Multiblock Copolymers of N, N-Dimethylacrylamide and N-Isopropylacrylamide, Langmuir 23 (2007) 13076–13084, https://doi.org/10.1021/la702548h.
[17] A. Vagias, A. Papagiannopoulos, L.P. Kreuzer, D. Giaouzi, S. Busch, S. Pispas, P. Müller-Buschbaum, Effects of Polymer Block Length Asymmetry and Temperature on the Nanoscale Morphology of Thermoresponsive Double Hydrophilic Block Copolymers in Aqueous Solutions, Macromolecules 54 (2021) 7298–7313, https://doi.org/10.1021/acs.macromol.1c01005.
[18] Z. Cao, W. Liu, P. Gao, K. Yao, H. Li, G. Wang, Toward an understanding of thermoresponsive transition behavior of hydrophobically modified N-isopropylacrylamide copolymer solution, Polymer 46 (2005) 5268–5277, https://doi.org/10.1016/j.polymer.2005.04.050.
[19] A. Baranowska-Korczyc, E. Stelmach, B. Paterczyk, K. Maksymiuk, A. Michalska, Ultrasmall self-assembly poly(N-isopropylacrylamide-butyl acrylate) (polyNIPAM-BA) thermoresponsive nanoparticles, J. Colloid Interface Sci. 542 (2019) 317–324, https://doi.org/10.1016/j.jcis.2019.02.004.
[20] V.D. Lechuga-Islas, G. Festag, M. Rosales-Guzmán, O.E. Vega-Becerra, R. Guerrero-Santos, U.S. Schubert, C. Guerrero-Sánchez, Quasi-block copolymer design of quaternized derivatives of poly(2-(dimethylamino)ethyl methacrylate): Investigations on thermo-induced self-assembly, Eur. Polym. J. 124 (2020) 109457, https://doi.org/10.1016/j.eurpolymj.2019.109457.
[21] M.T. Savoji, S. Strandman, X.X. Zhu, Block Random Copolymers of N-Alkyl-Substituted Acrylamides with Double Thermosensitivity, Macromolecules 45 (2012) 2001–2006, https://doi.org/10.1021/ma2027269.
[22] N. Migliore, A. Guzik, M.C.A. Stuart, M. Palà, A. Moreno, G. Lligadas, P. Raffa, Lactic Acid-Derived Copolymeric Surfactants with Monomer Distribution Profile-Dependent Solution and Thermoresponsive Properties, ACS Sustain. Chem. Eng. 10 (2022) 14806–14816, https://doi.org/10.1021/acssuschemeng.2c04354.
[23] K. Otake, H. Inomata, M. Konno, S. Saito, Thermal analysis of the volume phase transition with N-isopropylacrylamide gels, Macromolecules 23 (1990) 283–289, https://doi.org/10.1021/ma00203a049.
[24] J.E. Chung, M. Yokoyama, K. Suzuki, T. Aoyagi, Y. Sakurai, T. Okano, Reversibly thermo-responsive alkyl-terminated poly(N-isopropylacrylamide) core-shell micellar structures, Colloids Surf. B Biointerfaces 9 (1997) 37–48, https://doi.org/10.1016/S0927-7765(97)00015-5.
[25] Y. Xia, N.A.D. Burke, H.D.H. Stöver, End Group Effect on the Thermal Response of Narrow-Disperse Poly(N-isopropylacrylamide) Prepared by Atom Transfer Radical Polymerization, Macromolecules 39 (2006) 2275–2283, https://doi.org/10.1021/ma0519617.
[26] S. Furyk, Y. Zhang, D. Ortiz-Acosta, P.S. Cremer, D.E. Bergbreiter, Effects of end group polarity and molecular weight on the lower critical solution temperature of poly(N-isopropylacrylamide), J. Polym. Sci. Part Polym. Chem. 44 (2006) 1492–1501, https://doi.org/10.1002/pola.21256.
[27] M.L. Ohnsorg, J.M. Ting, S.D. Jones, S. Jung, F.S. Bates, T.M. Reineke, Tuning PNIPAm self-assembly and thermoresponse: roles of hydrophobic end-groups and hydrophilic comonomer, Polym. Chem. 10 (2019) 3469–3479, https://doi.org/10.1039/C9PY00180H.
[28] X.-P. Qiu, F. Tanaka, F.M. Winnik, Temperature-Induced Phase Transition of Well-Defined Cyclic Poly(N-isopropylacrylamide)s in Aqueous Solution, Macromolecules 40 (2007) 7069–7071, https://doi.org/10.1021/ma071359b.
[29] P.A. FitzGerald, S. Gupta, K. Wood, S. Perrier, G.G. Warr, Temperature- and pH-Responsive Micelles with Collapsible Poly(N-isopropylacrylamide) Headgroups, Langmuir 30 (2014) 7986–7992, https://doi.org/10.1021/la501861t.
[30] S.E. Kirkland, R.M. Hensarling, S.D. McConaughy, Y. Guo, W.L. Jarrett, C. L. McCormick, Thermoreversible Hydrogels from RAFT-Synthesized BAB Triblock Copolymers: Steps toward Biomimetic Matrices for Tissue Regeneration, Biomacromolecules 9 (2008) 481–486, https://doi.org/10.1021/bm700968t.
[31] C. Zhou, M.A. Hillmyer, T.P. Lodge, Efficient Formation of Multicompartment Hydrogels by Stepwise Self-Assembly of Thermoresponsive ABC Triblock Terpolymers, J. Am. Chem. Soc. 134 (2012) 10365–10368, https://doi.org/10.1021/ja303841f.
[32] M. Onoda, T. Ueki, R. Tamate, A.M. Akimoto, C.C. Hall, T.P. Lodge, R. Yoshida, Precisely Tunable Sol-Gel Transition Temperature by Blending Thermoresponsive ABC Triblock Terpolymers, ACS Macro Lett. 7 (2018) 950–955, https://doi.org/10.1021/acsmacrolett.8b00477.
[33] N. Morimoto, F. Segui, X.-P. Qiu, K. Akiyoshi, F.M. Winnik, Heat-Induced Flower Nanogels of Both Cholesterol End-Capped Poly(N-isopropylacrylamide)s in Water, Langmuir 38 (2022) 5218–5225, https://doi.org/10.1021/acs.langmuir.1c02394.
[34] L. Despax, J. Fitremann, M. Destarac, S. Harrisson, Low concentration thermoresponsive hydrogels from readily accessible triblock copolymers, Polym. Chem. 7 (2016) 3375–3377, https://doi.org/10.1039/C6PY00499G.
[35] F. Yin, J.S. Behra, M. Beija, A. Brûlet, J. Fitremann, B. Payré, S. Gineste, M. Destarac, N. Lauth-de Viguerie, J.-D. Marty, Effect of the microstructure of n-butyl acrylate/N-isopropylacrylamide copolymers on their thermo-responsiveness, self-organization and gel properties in water, J. Colloid Interface Sci. 578 (2020) 685–697, https://doi.org/10.1016/j.jcis.2020.06.005.
[36] S. Eggers, T. Eckert, V. Abetz, Double thermoresponsive block–random copolymers with adjustable phase transition temperatures: From block-like to gradient-like

behavior, J. Polym. Sci. Part Polym. Chem. 56 (2018) 399–411, https://doi.org/10.1002/pola.28906.
[37] J. Zhang, B. Farias-Mancilla, M. Destarac, U.S. Schubert, D.J. Keddie, C. Guerrero-Sanchez, S. Harrisson, Asymmetric Copolymers: Synthesis, Properties, and Applications of Gradient and Other Partially Segregated Copolymers, Macromol. Rapid Commun. 39 (2018) 1800357, https://doi.org/10.1002/marc.201800357.
[38] R. Yañez-Macias, I. Kulai, J. Ulbrich, T. Yildirim, P. Sungur, S. Hoeppener, R. Guerrero-Santos, U.S. Schubert, M. Destarac, C. Guerrero-Sanchez, S. Harrisson, Thermosensitive spontaneous gradient copolymers with block- and gradient-like features, Polym. Chem. 8 (2017) 5023–5032, https://doi.org/10.1039/C7PY00495H.
[39] K.-I. Seno, I. Tsujimoto, S. Kanaoka, S. Aoshima, Synthesis of various stimuli-responsive gradient copolymers by living cationic polymerization and their thermally or solvent induced association behavior, J. Polym. Sci. Part Polym. Chem. 46 (2008) 6444–6454, https://doi.org/10.1002/pola.22953.
[40] K.C. Gallow, Y.K. Jhon, J. Genzer, Y.-L. Loo, Influence of gradient strength and composition profile on the onset of the cloud point transition in hydroxyethyl methacrylate/dimethylaminoethyl methacrylate gradient copolymers, Polymer 53 (2012) 1131–1137, https://doi.org/10.1016/j.polymer.2012.01.027.
[41] N. Merlet-Lacroix, E.D. Cola, M. Cloitre, Swelling and rheology of thermoresponsive gradient copolymer micelles, Soft Matter 6 (2010) 984–993, https://doi.org/10.1039/B918854A.
[42] M. Bozorg, B. Hankiewicz, V. Abetz, Solubility behaviour of random and gradient copolymers of di- and oligo(ethylene oxide) methacrylate in water: effect of various additives, Soft Matter 16 (2020) 1066–1081, https://doi.org/10.1039/C9SM02032B.
[43] J.-S. Park, K. Kataoka, Precise Control of Lower Critical Solution Temperature of Thermosensitive Poly(2-isopropyl-2-oxazoline) via Gradient Copolymerization with 2-Ethyl-2-oxazoline as a Hydrophilic Comonomer, Macromolecules 39 (2006) 6622–6630, https://doi.org/10.1021/ma0605548.
[44] K. Nieswandt, P. Georgopanos, M. Held, E. Sperling, V. Abetz, RAFT Emulsion Polymerization of Styrene Using a Poly((N, N-dimethyl acrylamide)-co-(N-isopropyl acrylamide)) mCTA: Synthesis and Thermosensitivity, Polymers 14 (2022) 62, https://doi.org/10.3390/polym14010062.
[45] A.V. Feoktystov, H. Frielinghaus, Z. Di, S. Jaksch, V. Pipich, M.-S. Appavou, E. Babcock, R. Hanslik, R. Engels, G. Kemmerling, H. Kleines, A. Ioffe, D. Richter, T. Brückel, KWS-1 high-resolution small-angle neutron scattering instrument at JCNS: current state, J. Appl. Crystallogr. 48 (2015) 61–70, https://doi.org/10.1107/S1600576714025977.
[46] M. Daoud, J.P. Cotton, Star shaped polymers: a model for the conformation and its concentration dependence, J. Phys. 43 (1982) 531–538, https://doi.org/10.1051/jphys:01982004303053100.
[47] A.J. Convertine, B.S. Lokitz, Y. Vasileva, L.J. Myrick, C.W. Scales, A.B. Lowe, C. L. McCormick, Direct Synthesis of Thermally Responsive DMA/NIPAM Diblock and DMA/NIPAM/DMA Triblock Copolymers via Aqueous, Room Temperature RAFT Polymerization, Macromolecules 39 (2006) 1724–1730, https://doi.org/10.1021/ma0523419.
[48] J. Ma, C. Guo, Y. Tang, H. Liu, 1H NMR Spectroscopic Investigations on the Micellization and Gelation of PEO−PPO−PEO Block Copolymers in Aqueous Solutions, Langmuir 23 (2007) 9596–9605, https://doi.org/10.1021/la701221f.
[49] E. Christ, D. Collin, J.-P. Lamps, P.J. Mésini, Variable temperature NMR of organogelators: the intensities of a single sample describe the full phase diagram, Phys. Chem. Chem. Phys. 20 (2018) 9644–9650, https://doi.org/10.1039/C8CP00009C.
[50] W.D. Dozier, J.S. Huang, L.J. Fetters, Colloidal nature of star polymer dilute and semidilute solutions, Macromolecules 24 (1991) 2810–2814, https://doi.org/10.1021/ma00010a026.